Title: The early local and systemic Type I interferon responses to ultraviolet B light exposure are cGAS dependent.

Authors:

Sladjana Skopelja-Gardner[1], Jie An[1], Joyce Tai[1], Lena Tanaka[1], Xizhang Sun[1], Payton Hermanson[1], Masaoki Kawasumi[2], Richard Green[3,4], Michael Gale, Jr.[3,4], Andrea Kalus[2], Victoria P. Werth[5], Keith B. Elkon[1,3,4]

Affiliations: [1]Division of Rheumatology, [2]Division of Dermatology, [3]Department of Immunology, and [4] Center for Innate Immunity and Immune Disease, University of Washington, Seattle, WA, USA, and [5]Dermatology Section, Philadelphia Veterans Affairs Medical Center, Philadelphia, USA.

Corresponding Author:

Keith B. Elkon, Division of Rheumatology, University of Washington, 750 Republican Street E531, Seattle, Washington 98109, USA. Phone: 206.616.5636; E-mail: KElkon@medicine.washington.edu

Abstract

Most systemic lupus erythematosus (SLE) patients are photosensitive and ultraviolet B light (UVB) exposure worsens cutaneous disease and precipitates systemic flares. The pathogenic link between skin disease and systemic exacerbations in SLE remains elusive. Since the type I interferon (IFN-I) signature is detected in both the blood and skin of SLE patients and because cell injury through radiation therapy activates the cytosolic DNA sensor, cGAS, we asked whether UVB stimulated IFN-I through the cGAS pathway *in vivo*. In an acute model of UVB-triggered inflammation, we observed that a single exposure triggered an IFN-I signature not only in the skin, but also in the blood and kidneys. Early IFN-I response in the skin was almost entirely, and in the blood partly, dependent on the presence of cGAS, as was skin inflammation. Inhibition of cGAMP hydrolysis augmented the UVB-triggered IFN-I response. UVB skin exposure leading to cGAS-activation and IFN-I production could contribute to acute flares of disease in SLE.

Introduction

Skin sensitivity to ultraviolet B (UVB) light affects ~70-85% of systemic lupus erythematosus (SLE) patients and results in both localized cutaneous disease as well as systemic disease flares (Foering et al., 2012; Zeidi et al., 2019). How photosensitivity leads to systemic disease exacerbations in SLE is unknown. We previously showed that repetitive exposure of mice to low doses (100 mJ/cm^2) of UVB light triggered IFN-I response in the skin (Sontheimer et al., 2017), a result recently confirmed by Wolf et al (Wolf et al., 2019). However, we observed that expression of type I interferon (IFN-I) signature genes (ISG) in the skin was blunted in mice deficient in the DNA sensing adapter, STING (stimulator of interferon genes) (Sontheimer et al., 2017). Since cGAS is the most prominent DNA sensor leading to STING activation and this pathway is activated following UV light exposure of cells *in vitro* and gamma irradiation *in vivo* (Deng et al., 2014; Kemp et al., 2015; Vanpouille-Box et al., 2017), we addressed whether cGAS was necessary for the *in vivo* IFN-I response to UV light. We also compared the responses in male and female mice, since SLE is a female dominant disease (Christou et al., 2019). We subsequently explored the effects of cGAS-STING activation on the IFN-I and inflammatory responses locally (skin) and systemically (blood and kidneys) and found that cGAS was necessary for the early IFN-I response to UVB. UVB exposure of normal humans also induced an IFN-I signature demonstrating the translational relevance of these studies.

Results and Discussion

A single exposure to UVB light triggers an early cutaneous IFN-I response exaggerated in female mice.

In vitro and *ex vivo* studies reported that UVB and UVC light-mediated cell damage induced IFN-I in keratinocytes and other cell types (Gehrke et al., 2013; Sarkar et al., 2018), possibly aided by the downregulation of ULK-1, a STING inhibitor (Kemp et al., 2015). We and others observed that repeated exposure to low doses of UVB light (100mJ/cm^2 per day for 5 days) caused a modest upregulation in ISG expression in the skin of normal mice (Sontheimer et al., 2017; Wolf et al., 2019). However, this subacute model generates cycles of inflammation and resolution, which complicates understanding as to whether IFN-I reflects immediate injury or a wound repair response. Here, we first addressed whether a single high dose (500mJ/cm^2 in all experiments) of UVB light *in vivo* affects IFN-I production in C57BL/6J (B6) mice, a strain shown to best mirror cutaneous changes to UVB in human skin (Sharma et al., 2011). This, or higher doses have been widely used in the B6 mice and defined as 2 minimal inflammatory doses (Bernard et al., 2012; Patra et al., 2019).

Gene expression analyses of skin at different times (6, 24, and 48 hours) following exposure to a single dose of UVB light demonstrated a striking increase (~10-fold) in cutaneous ISG mRNA levels: *Irf7, Ifit1, Ifit3, Ifi44, Isg15, Isg20,* and *Mx1*, compared to non-UV exposed baseline (**Fig. 1A**). The mRNA expression levels of the majority of the tested ISG remained above baseline (1.8-16 fold induction) 48hr after exposure to UVB light, demonstrating that UVB-triggered IFN-I signaling persisted for several days (**Fig. 1A**). Similar to a previous report using *ex vivo* samples (Sarkar et al., 2018), we detected a modest (~2-fold) and transient (6 hr) IFN-κ expression in the skin (not shown). Early induction in cutaneous expression of all the tested ISG was strikingly higher in female than in male mice, and the greater fold-induction of some ISG in female skin persisted at 24hr (*Ifit3 and Ifif44)* and 48hr (*Ifit3* and *Irf7)* after UVB exposure (**Fig. 1A**). Skin IFN scores (**Fig. 1B**), i.e. composite scores of the relative expression of each gene at specific time points relative to the baseline levels prior to UVB injury (Feng et al., 2006), were higher in female compared to age matched male mice (mean IFN scores in female vs. male skin: 6hr = 8.56 vs. 1.0, 24hr = 8.7 vs. 3.6, 48hr = 4.9 vs. 2, **Fig. 1B**). These data demonstrate that females exhibit a markedly exaggerated early cutaneous IFN-I response to UVB injury (as much as 10-fold compared to males at 6hr), which is consistent with the more 'pro-inflammatory' nature of female skin proposed by Liang et al (Liang et al., 2017). The greater ISG response in the skin in females is not restricted to the UV light response, as females had higher ISG expression in

response to HIV infection, possibly contributing to a greater protective role at the epithelial and mucosal surfaces (Chang et al., 2013). In light of these findings, all subsequent experiments were performed using female mice.

To test the relevance of our acute model of UV light-triggered IFN-I response in human skin, we exposed healthy volunteers (n=5, female) to a single dose of UV light (2 MED for UVB) and performed RNA sequencing on skin biopsies from unexposed skin and skin collected 6hr and 24hr after UV exposure. Using a published set of IFN-I response genes (Der et al., 2019), we demonstrated that a single UV exposure triggered an IFN-I signature in healthy skin as early as 6hr (**Fig. 1C-D**). Analogous to the murine studies, we observed a prominent IFN-I signature after UV exposure even when only the 7 genes investigated in the mouse skin were used to derive the IFN-I scores (**Fig. 1E**). Notably, the IFN-I scores derived from the 7 genes made up ~30% of the total IFN-score generated from the entire gene set (188 IFN-I response genes, **Fig. 1D-E**), suggesting that the 7 ISGs investigated in the murine studies are a reasonable representation of the overall IFN-I response in the human skin. These data for the first time demonstrate that UV light stimulates an IFN-I response in the human skin *in vivo.* Although it is well established that most SLE patients demonstrate an IFN-I signature in affected and unaffected skin (Der et al., 2017; Farkas et al., 2001), the genesis of ISGs in the skin is unknown. Our findings suggest UV light as a potentially important source of IFN-I activation in the skin in humans as well as mice.

cGAS is essential for the early cutaneous IFN-I response after UVB light-mediated injury.

UV light is genotoxic, cytotoxic, and generates modified nucleic acids such as oxidized DNA (Gehrke et al., 2013). Recently, we discovered that IFN-I and inflammatory cytokines induced by UVB light were markedly reduced in STING deficient mice (Sontheimer et al., 2017). Canonically, STING has been thought to act primarily as a cytosolic DNA sensing adaptor protein downstream of cGAS. Upon engaging the cGAS synthesis product 2'3' cGAMP, STING undergoes a conformational change to bind TANK binding kinase 1 (TBK1) and enable the phosphorylation of interferon regulatory factor 3 (IRF3) as well as activation of IKKβ and NFκB, leading to production of IFN-I and inflammatory cytokines, respectively (Dunphy et al., 2018). However, other DNA (AIM2, IFI16, DAI) as well as RNA sensors (RIG-I-MAVS) signal through or cooperate with STING to drive IFN-I production in certain viral infections (Dunphy et al., 2018; Zevini et al., 2017). Whether skin inflammation triggered by UV light triggers DNA to activate the canonical cGAS-STING pathway *in vivo* is unknown. We therefore compared the ISG mRNA expression levels 6 and 24 hours following a single UVB light exposure of age-matched female B6 (wild type, WT) or *cGAS-/-* B6 mice. It should be noted that signaling by TLR and other sensors are not impaired in

cGAS-deficient mice (Wu et al., 2013). Whereas no difference in baseline (no UVB) skin ISG mRNA levels was found between WT and *cGAS-/-* mice (not shown), we observed that cGAS deficiency almost completely abrogated the early (6hr) cutaneous ISG expression after exposure to UVB (**Fig. 2A**). The lack of early ISG induction in *cGAS-/-* mice was comparable to that of IFN-α/β receptor deficient controls (*Ifnar-/-*) (**Fig. 2B).** While ISG expression in the *cGAS-/-* skin was detected 24hr after exposure to UVB, the fold-increase in ISG levels was substantially diminished compared to WT controls (45.7% (*Ifit1)*- 84.1% (*Ifit3)* reduction) (**Fig. 2A**). However, ISG mRNA levels in *cGAS-/-* skin were significantly higher than in *Ifnar-/-* controls at this later time point (**Fig. 2A**). Cumulative skin IFN scores confirmed that cGAS was required for the early cutaneous IFN signature after UVB injury, as ISG expression was not increased in cGAS-/- mice at 6hr. While later IFN-I scores in cGAS-deficient mice were lower than those in WT skin, they were significantly higher than in the *Ifnar-/-* controls (**Fig. 2B**), indicating that cGAS-independent pathways contributed to the IFN signature in the skin exposed to UV light over time. At this later time point, a modest increase in some ISGs (*Ifit1*, *ifi44,* Fig. 2A) in *Ifnar-/-* mice is consistent with previous reports of IFN-independent activation of these particular genes through IRF3-mediated gene expression (Ashley et al., 2019; Green et al., 2018). Together, these data confirm that the requirement for cGAS in the cutaneous IFN-I response to UVB is temporally regulated: i) cGAS is essential for the early activation of IFN-I signaling and ii) the cGAS-STING pathway is the dominant but not sole contributor to IFN-I activation in the skin later (24hr) following exposure to UVB. Similar temporarily distinct roles for different DNA and RNA sensors have been described in virus infections. For example, following HSV1 infection, both cGAS and IFI16 were required for the early (6hr) IFNβ or TNF response but RIG-I was necessary for cytokine production at a later time point (16hr) (Chiang et al., 2018).

Since export of the cGAS product, cGAMP, plays a role in the induction of IFN-I following radiation therapy (Ablasser et al., 2013; Bakhoum et al., 2018; Chen et al., 2016), we asked whether release of cGAMP following UVB radiation injury impacts IFN-I stimulation in the skin. To address this question, we inhibited the cell surface membrane enzyme ectonucleotide pyrophosphatase phosphodiesterase 1 (ENPP1), which hydrolyzes cGAMP (Carozza et al., 2019; Li et al., 2014), shortly before skin exposure to UVB (**Fig. 2C**). The ENPP1 inhibitor, STF-1084, (Carozza et al., 2019) led to a significantly greater induction in individual ISG expression as well as the cumulative IFN scores, compared to both the vehicle-treated skin exposed to UVB as well as to the unexposed skin treated with the ENPP1 inhibitor (**Fig. 2D-E**). These data suggest that UVB exposure exaggerated cGAMP release which, in turn, amplified the IFN signature.

UV irradiation triggers a number of biologic pathways in the skin including DNA damage, DNA repair, cell death, inflammation, and resolution of skin damage and repair (Schuch et al., 2017; Yamazaki et al., 2018). Pathways of DNA damage and repair are complex and have been examined in response to UV light and ionizing radiation (Bashir et al., 2009). The inflammatory cytokine response in mouse skin includes increased expression of TNF, IL-6 and IL-1β (Bashir et al., 2009; Bernard et al., 2012). Since the cGAS-STING pathway has been implicated in the regulation of these inflammatory cytokines through NFκB-mediated transcriptional activation or by activation of the inflammasome and generation of IL-1β (Abe and Barber, 2014; Swanson et al., 2017), we next asked whether UVB-triggered cGAS activation is necessary to induce these cytokines. We found that a single high dose of UVB light induced rapid expression (6hr) of TNF, IL-6, and IL-1β but that the extent of the TNF and IL-6 response was equivalent in wild-type and *cGAS-/-* mice (**Fig. 2F**). These findings suggest that the cGAS-STING pathway predominantly activates IRF-3 in UV light injured skin, while other pathways provide the main source of NF-κB signaling in this context. Two pathways stand out as possible contributors to this early inflammatory cytokine response as well as the later IFN-I response: TLR-3, which was responsible for stimulating TNF production in response to UV light-triggered RNA damage (Bernard et al., 2012), and ATM-IFI16-STING, which predominantly activated NF-kB and IL-6 production in response to etoposide DNA damage (Dunphy et al., 2018). In contrast to TNF and IL-6, IL-1β mRNA levels were significantly lower in *cGAS-/-* skin both 6 and 24hr after UVB exposure (**Fig. 2F**). While the relationship between IFN-I and IL-1β is complex, cGAMP can prime and activate the NLRP3 inflammasome (Gaidt et al., 2017; Swanson et al., 2017) likely explaining why IL-1β is lower in cGAS deficient compared to WT mice following exposure to UVB. A significant reduction in IL1-β gene expression was also detected in IFNAR deficient mice, suggesting that intact IFN-I signaling is important for inflammasome activation following UV light injury (**Fig. 2F**).

Skin exposure to UVB light triggers a systemic IFN-I response

The presence of an IFN signature in SLE patients was first detected in peripheral blood mononuclear cells (PBMC) in 2003 (Baechler et al., 2003; Bennett et al., 2003; Crow et al., 2003). More recently, the IFN signature in PBMC was reported in patients with cutaneous lupus (Braunstein et al., 2012) and the IFN signature in SLE skin has been linked to a similar signature in lupus nephritis (Der et al., 2017; Der et al., 2019). A key question in SLE is whether the IFN signature detected in PBMC is generated in blood or in tissues and, if in tissues, which tissues are responsible? To address this question experimentally, we exposed mice to the single dose of UVB light and quantified ISG expression in blood cells. As shown in **Fig. 3A**, UVB light-mediated

skin injury triggered a striking upregulation in ISG mRNA levels in the peripheral blood cells (6-24hr). Compared to the skin, where ISG expression persisted 24hr after exposure to UVB (Fig. 2), the kinetics of ISG expression in the blood varied. Expression levels of most genes peaked early while others were higher at 24hr (*Isg15* and *Isg20*) after UVB injury (Fig. 3A), possibly reflecting a second wave of injury, infiltration of immune cells, different DAMPs, or other mechanisms.

Similar to the findings in the skin, early ISG expression in peripheral blood was largely abrogated in cGAS deficient mice (by 45.1% (*Ifit1)* - 95% (*Ifi44)*), as well as in the absence of the IFNAR (~93% decrease), although the extent to which specific ISGs were affected differed (**Fig. 3A**). At 24hr after UVB injury, the expression levels of the majority of ISGs upregulated in WT mice were lower in the blood of cGAS-/- animals (by 57% (*Mx1)*- 88% (*Usp18)*, **Fig. 3A**). To average the differences in the UV light-stimulated IFN signature in the 3 genotypes, we calculated the blood IFN scores using expression levels of 7 ISGs. Overall, cGAS deficient mice demonstrated significantly lower blood IFN-I scores than their cGAS-sufficient counterparts, at both 6 and 24hr after UV light exposure (**Fig. 3B**). Blood cell IFN-I scores in *cGAS*-/- mice were higher than in the *Ifnar*-/- controls at 24hr post exposure indicating that other sensors besides cGAS also played a role at this time (**Fig. 3B**). Of relevance to human SLE, pre-treatment of mice with hydroxychloroquine (HCQ), a TLR and cGAS antagonist (An et al., 2015) that has demonstrated efficacy in treating cutaneous lupus in patients with an IFN signature (Chang et al., 2011), significantly decreased the early IFN-I scores in both the skin and the blood in B6 mice after exposure to UVB light (**Fig. 3C**).

Consistent with activation of the cGAS-STING pathway and failure to detect pDC in short term experiments (Sontheimer et al., 2017) and confirmed here (not shown), exposure to UVB light triggered an early increase in the circulating levels of IFNβ in WT mice (**Fig. 3D**). A robust increase (~50%) in expression of Sca-1, a cell surface protein marker that reflects exposure to IFN-I (DeLong et al., 2018) on B cells, the blood cell with the highest IFNAR levels (Pogue et al., 2004), confirmed the release of IFN-I into the circulation following skin exposure to UVB in WT mice (**Fig. 3E**). Consistent with the lack of the IFN signature early in the blood of cGAS-/- mice (Fig. 3B), we could not detect an increase in the levels of circulating IFNβ (**Fig. 3D**) or upregulation of Sca-1 expression on cGAS deficient B cells (**Fig. 3E**). Therefore, in addition to the cutaneous response, a single exposure to UVB light stimulated an early cGAS-dependent IFN-I response in the blood. Together, these findings strongly suggest an important role for IFNβ in UV-light triggered IFN-I response. While IFNβ has been difficult to detect in circulation, likely due to its very high affinity for the IFNAR (20-30 fold higher than IFNα, (Ng et al., 2016)), recent analysis of

the IFN signature in the skin of SLE patients identified a predominantly IFNβ driven gene response (Catalina et al., 2019). IFNβ may also be produced by B cells from SLE patients (Hamilton et al., 2018) and appears to be required for the development of autoreactive B cells in a mouse lupus model (Hamilton et al., 2017). While pDC have been detected in the skin of SLE patients with established disease (Farkas et al., 2001) and are considered major producers of IFNα following TLR7 or TLR9 activation (Barrat et al., 2005), they can also be the source of IFNβ through cGAS-STING activation (Bode et al., 2016).

In line with recent reports that the presence of an IFN signature in keratinocytes associates with lupus nephritis, as well as with an IFN-I response in the kidney tissue (Der et al., 2017; Der et al., 2019), we observed an increase in ISG and Sca-1 expression levels in kidneys 24hr after skin exposure to UVB (**Fig. 3F-G**). Since the kidneys had been perfused to remove circulating blood cells, the IFN signature is likely explained by the direct influence of IFNβ or DAMPs on kidney resident cells or due to tissue infiltration of IFNβ producing cells migrated from the blood after skin exposure to UVB. These data reinforce the notion that skin might act as a source or origin of the systemic IFN-I in SLE, which is further supported by recent findings showing a 480-fold increase in ISG expression in non-lesional skin versus only a 7.8-fold increase in the blood relative to healthy controls (Psarras et al., 2018). Intriguingly, individuals at-risk for developing SLE (ANA+, treatment naïve, $\leq$1 clinical criteria) also present with a skin (28.7-fold increase) and a smaller blood IFN signature (2.2 fold increase) (Psarras et al., 2018).

Absence of cGAS dampens the cellular inflammatory response in UV light-exposed skin

Analogous to inflammation triggered by infection (Bogoslowski et al., 2018) and our observations of UVB light mediated sterile inflammation in the subacute model (Sontheimer et al., 2017), the acute response to UVB light in the skin was characterized by infiltration of neutrophils as well as inflammatory monocytes (CD11b+Ly6C^{high}) to the site of injury (**Fig. 4A-B**). Besides innate immune cells, exposure to UVB triggered an increase in the number of CD8+ and γδ+ (**Fig. 4C-D)** but not CD4+ (not shown) T cells in the skin of WT mice. The number of both myeloid as well as T cell populations early (6hr) after UVB exposure was significantly reduced in the skin of cGAS-deficient mice (**Fig. 4A-D**). The diminished skin infiltration of inflammatory monocytes and CD8+ T cells in *cGAS-/-* mice was sustained 24hr after UVB exposure (**Fig. 4B-C**). Therefore, in addition to driving both the local and the systemic acute IFN-I response, cGAS-mediated DNA sensing also regulates the magnitude of the cellular infiltration into UV light-injured skin.

The ability of the cGAS-STING pathway to shape the inflammatory response via IFN-I signaling was recently identified in both spontaneous and therapy-induced anti-tumor immunity

(Li et al., 2019; Vatner and Janssen, 2019). The muted T cell response we observed in the absence of cGAS was analogous to the findings in the anti-tumor response, where cGAS-STING activation was required for the recruitment of tumor specific CD8+ T cells and their infiltration into the tumor environment (Harding et al., 2017; Ohkuri et al., 2014; Wang et al., 2017). These effects were largely attributed to the IFN-I response gene CXCL10, a recognized CD8+ T cell chemoattractant (Christensen et al., 2006; Li et al., 2019; Liu et al., 2015). Indeed, we found decreased CXCL10 expression in the skin of cGAS-deficient mice both early and 24hr after exposure to UVB (**Fig. 4E**). The role of cGAS in innate immune cell recruitment is less well established. The reduction in neutrophil infiltration into the skin in cGAS-deficient mice could be due to diminished production of IL-1β (**Fig. 2F**) or reduced early expression of CXCL1 (**Fig. 4F),** whereas lower cutaneous CCL2 expression in *cGAS-/-* mice (**Fig. 4G**) could explain the reduced monocyte numbers in skin. Together, our data indicate that DNA sensing by cGAS contributes to innate and adaptive immune cell recruitment to UVB light exposed skin, either directly through IFN-I signaling, via inflammasome activation, or via additional pathways of inflammatory chemokine regulation.

Concluding remarks

In this *in vivo* study of the effects of an acute exposure to UVB light, we reveal a number of novel findings. A single dose of UVB stimulates a robust IFN-I response in both murine and human skin, which, in the early phase (6hr) in mice, is entirely cGAS dependent and is heightened in females. Remarkably, UVB exposure induces a systemic IFN-I response as determined by IFN signatures in the blood and kidney. The early blood IFN-I response is dependent on cGAS and is inhibited by hydroxychloroquine which is consistent with our findings that aminoquinoline antimalarial drugs inhibit the cGAS activity *in vitro* and *in vivo* (An et al., 2018; An et al., 2015). Finally, we demonstrate that the absence of cGAS leads to diminished inflammatory response to UV light, including decreased chemokine expression and reduced numbers of innate and adaptive immune cells into the UV light-exposed skin.

The detection of an IFN signature in the blood in SLE patients was a landmark discovery but where and how IFN-I is generated is not known. Here, we show that a single dose of UV light can generate an IFN signature in the blood of normal mice. Since ~70-85% of SLE patients are photosensitive and the skin has a vast surface area, it is plausible that IFN-I generated in the skin through activation of cGAS-STING and released into the circulation is, at least in part, responsible for the blood IFN signature in SLE patients. Whether UVB- triggered release of DAMPs, diffusion of IFNβ, or cell trafficking is responsible for the blood IFN signature remains to be determined.

In the last 6 years, the cytosolic DNA sensing cGAS-STING pathway has been implicated in innate immune and adaptive IFN-I responses to viral infections, inflammatory cell death, tumor cell-derived DNA, as well as DNA damage triggered by chemo- or radiation therapy in tumors (Li and Chen, 2018; Lood et al., 2016). Here, we observed that both local and systemic early production of IFN-I following skin exposure to UVB was almost entirely cGAS dependent. In normal situations, acute inflammation is resolved through many reparative mechanisms that involve T-regulatory cells, Langerhans cells, and anti-inflammatory cytokines such as IL-10 (Shipman et al., 2018; Wolf et al., 2019; Yamazaki et al., 2018). Why SLE patients fail to control the inflammatory response in the skin and elsewhere is a critical question that will benefit from understanding the pathogenetic pathways involved.

Materials and Methods

Mice and UV irradiation

Male and female 12-16 week old C57BL/6 (B6, wild type), B6.*cGAS-/-*, or B6.*Ifnar-/-* mice were shaved dorsally. Mice were anesthetized with isoflurane and a single dose of UVB (500 mJ/cm^2) was delivered either to the whole (figure 1) or half of the back (figures 2-5) using FS40T12/UVB bulbs (National Biological Corporation). The UVB light energy at the dorsal surface was measured with Photolight IL1400A radiometer with a SEL240/UVB detector (International Light Technologies). All animal experiments were approved by the Institutional Animal Care and Use Committee of the University of Washington, Seattle. Mutant mice were kindly provided by Drs. Daniel Stetson and Michael Gale at the University of Washington.

Detection of Interferon Stimulated Gene (ISG) Expression and IFNβ production

Skin biopsies (6mm) were performed prior to irradiation and at different time points after acute UVB injury: 6, 24, and 48 hours and tissue stored in RNA Later solution (Qiagen). Whole blood was collected prior to, 6hr, and 24hr following UVB light irradiation and red blood cells lysed. Kidneys were collected from mice following whole body cardiac perfusion with saline (Bethunaickan and Davidson, 2012). RNA from skin and kidney was extracted by RNA Easy kit from Qiagen (Valencia, CA) and from blood cells using Quick RNA Miniprep (Zymogenetics). cDNA was synthesized using High Capacity cDNA synthesis kit (Applied Biosciences). ISG transcripts were selected according to previous studies of IFN response to UV and in *Trex-/-* animals (An et al., 2018; Sontheimer et al., 2017) and quantified by real time quantitative PCR (qPCR) and normalized to *18S* (skin) or *Gapdh* (blood) transcript levels, using the following primers: *Isg15,* F:5′-AAGCAGCCAGAAGCAGACTC-3′ and R:5′-CACCAATCTTCTGGGCAATC-3′*, Isg20* , F:5'- TCACGGA CTACAGAACCCAAG-3' and R: 5' –TATCCTCCTTCAGGGCATTG-3', IFN regulatory factor 7 (*Irf7*), F:5′-GTCTCGGCTTGTGCTTGTCT-3′ and R:5′-CCAGGTCCATGAGGAAGTGT-3′*, Mx1* F:5′-CCTCAGGCTAGATGGCAAG-3′ and R:5′ CCTCAGGCTAGATGGCAAG-3′*, Ifit1*, F:5′-TGCTGAGATG GACTGTGAGG-3′ and R:5′-CTCCACTTTCAGAGCCTTCG-3′*; Ifit3,* F:5'-TGGCCTACATAAAGCACCTAGATGG-3' and R:5'-CGCAAACTTTTGGCAAACTTGTCT-3'; *Ifi44,* F:5'-AACTGACTGCTCGCAATAATGT-3' and R:5'-GTAACACAGCAATGCCTCTTGT-3', *Usp18,* F*: 5'- TTGGGCTCCTGAGGAAACC-3' and* R*:5'- CGATGTTGTG TAAACCAACCAGA-3', Oasl1,* F*: 5'- CAGGAGCTGTACGGCTTCC-3' and* R*: 5'- CCTACCTTGAGTACCTTGAGCAC-3'. Ifi27l2a,* F*:5'- CTGTTTGGCTCTGCCATAGGAG-3' and* R*: 5'- CCTAGGATGGCATTTGTTGATGTGG-3', Gapdh,* F: 5'-

TGGAAAGCTGTGGCGTGAT-3' and R: 5'- TGCTTCACCACCTTCTTGAT-3', and *18s*, F: 5'-AACTTTCGATGGTAGTCGCCGT-3' and R: 5'-TCCTTGGATGTGGTAGCCGTTT-3'. Fold induction in ISG expression was determined using the standard formula $2^{(-\Delta\Delta Ct)}$ relative to baseline, i.e. skin prior to exposure to UVB. Mean IFN score was calculated as previously described (Braunstein et al., 2012): sum of normalized ISG expression levels; *i = each ISG;* SD = standard deviation.

$$\sum_{i=1}^{7} = \frac{Gene\ i_{6\ or\ 24hr} - mean\ Gene\ ipreUV}{SD\ (Gene\ ipreUV)}$$

Interferon beta (IFNβ) protein levels in plasma were measured using Legendplex Mouse Inflammation Panel (Biolegend).

Flow cytometry analysis of inflammation

Skin biopsies (1 6mm biopsy at 6hr and 5 6mm biopsies at 24hr) from female B6 and *cGAS-/-* mice were obtained prior to, 6hr, and 24hr after skin exposure to UVB light. Skin biopsies were processed as previously described (Sontheimer et al., 2017). Briefly, the tissue was minced finely and digested with 0.28 units/ml Liberase TM (Roche) and 0.1 mg/ml of Deoxyribonuclease I (Worthington) in PBS with Ca^{+2} and Mg^{+2} for 60 minutes at 37°C with shaking. Cells were passed through a 0.7 µm strainer, resuspended in RPMI and counted. Cell were treated with Fc Block TruStain FcX (Biolegend) and stained in PBS + 1% BSA. Surface staining was performed using mouse–specific fluorescent antibodies purchased from Biolegend: i) Myeloid panel: CD45 APC.Cy7, CD11b PerCP.Cy5.5, Ly6C Violet 610, Ly6G FITC and ii) T cell panel: CD45 APC.Cy7, CD8 PerCP.Cy5.5, CD4 Pe.Cy7, γδ T PE. Samples were processed using CytoFLEX flow cytometer (Beckman Coulter) and data analyzed with FlowJo software v10 (Tree Star). Mean fluorescence intensities (MFI) of Sca-1 as well as percent positive populations were determined using fluorescence minus one (FMO) controls. Numbers of different cell populations were determined based on total counted cell numbers and normalized to the area of a single biopsy (6 mm).

***In vivo* treatment with hydroxycloroquine (HCQ) and ENPP1 inhibitor**

Mice (B6) were treated with HCQ (25 mg/kg/day) for 3 weeks administered orally in Splenda-sweetened water. Controls were treated with Splenda-sweetened water alone. Following 3 weeks of treatment, mice were exposed to UVB light as described above. Blood and skin taken prior to and 6hr after UV exposure were analyzed for ISG expression by qPCR and IFN scores derived, as described above. For treatment with ENPP1 inhibitor, mice were injected intradermally with

50µl 100 µM STF1084 (two injections per mouse) (generously provided by Yinling Li at Stanford University), as used by Carozza et al for intra-tumoral injections (Carozza et al., 2019). After 30 minutes, mice were irradiated with a single dose of UVB light as described above. Skin biopsies were collected after 16hr and processed for RNA isolation and QPCR as above. Skin was analyzed for ISG expression under four different conditions: vehicle alone, STF-1084 alone, vehicle + UVB, and STF1084 + UVB. Fold change in ISG expression was determined relative to vehicle alone control skin. IFN scores were derived as described above.

Human phototesting and skin RNA Sequencing

Healthy volunteers were recruited by informed consent (HSD #50655) from the University of Washington (UW, Seattle WA) and Philadelphia Veterans Affairs Medical Center (Pennsylvania, PA). The sun-protected skin of 5 female healthy controls was exposed to two minimal erythematous doses (MED) of UVB light on the dorsal surface of the lower arm. Solar Simulator radiation was generated using a 150 W xenon arc, single port Berger Solar Simulator (Solar Light, Model # 16S-150/300, Glenside, PA). UG- 5 and WG 320/1inch thick glass filters was fitted to give a wavelength spectrum that includes wavelengths above 290nm-400nm. A 6-mm punch skin biopsy was collected from unexposed skin, and from skin 6hr and 24hr after UV exposure. Tissue was stored in RNA later and samples from PA shipped to UW. Following RNA isolation at UW, the RNA yield was 2-3 ug RNA (all samples had RIN >9.5). RNA sequencing was performed at Northwest Genomics Center at the University of Washington. cDNA libraries were prepared from 1 µg of total RNA using the TruSeq Stranded mRNA kit (Illumina, San Diego, CA) and the Sciclone NGSx Workstation (Perkin Elmer, Waltham, MA). Prior to cDNA library construction, ribosomal RNA was removed by means of poly-A enrichment. Each library was uniquely barcoded and subsequently amplified using a total of 13 cycles of PCR. Library concentrations were quantified using Qubit fluorometric quantitation (Life Technologies, Carlsbad, CA). Average fragment size and overall quality were evaluated with the DNA1000 assay on an Agilent 2100 Bioanalyzer. Each library was sequenced with paired-end 75 bp reads to a depth of 30 million reads on an Illumina HiSeq 1500 sequencer.

RNAseq Data Processing and Analysis

Raw RNAseq data (Fastq files) were demultiplexed and checked for quality (FastQC version 0.11.3). Next rRNA was digitally removed using Bowtie2 (version 2.2.5). Sufficient host reads (~thirty million) were then mapped to the Human genome (GRCh37) using STAR (2.4.2a) and then converted into gene counts with ht-seq (0.6.0). Both the genome sequence (fasta) and gene

transfer files (gtf) were obtained using Illumina's igenomes website (https://support.illumina.com/sequencing/sequencing_software/igenome.html). Gene counts were then loaded in the R statistical programming language (version 3.2.1) and filtered by a row sum of fifty or more across all samples. Raw fastq files and count matrix were submitted to GEO and available under accession GSEXXX. Exploratory analysis and statistics were also run using R and bioconductor. The gene count matrix was normalized using EDGER and transformed to log counts per million (logCPM) using the voom through the limma bioconductor package (3.24.15). Statistical analysis (including differential expression) was performed using the limma package (Smyth, 2004).

Interferon Z-score heatmap: Differential expression data was filtered for interferon genes and then plotted using the heatmap.2 function with the gplots bioconductor package in R (Gentleman et al., 2004).

IFN score analysis: IFN-I scores at 6 (n=3) and 24hr (n=5) after UV were derived using the established IFN-I response gene dataset (188 of 212 genes were detected (Der et al., 2019). Relative expression of genes at baseline (prior to UV, n=5) and at different times after UV was normalized as described above and IFN scores generated using the same formula as for mouse studies, using either all 188 genes or just the 7 genes used in mouse studies.

Statistical Analysis

Data were analyzed using GraphPad Prism 7 software (GraphPad Software Inc.) and presented as mean $\pm$ SEM. Statistical difference between two data groups was determined using Student's *t*-test. One way-ANOVA was used to determine statistical significance between three groups in human UV exposure studies. $P < 0.05$ was considered significant.

Acknowledgments:

This work was supported by National Institutes of Health R21 AR072377-01 and ACR Rheumatology Research Foundation Grant to Keith Elkon; Veterans Affairs Merit Review [I01BX000706] to VPW and NIH/NIAMS Werth R01AR071653. The RNA Sequencing work was supported by an NIH grant for the University of Washington Interdisciplinary Center for Exposures, Diseases, Genomics & Environment, P30ES07033. We thank Tomas Mustelin, Jeffrey Ledbetter, Edward Clark, and Erika Noss for insightful discussion. We thank Yinling Li at Stanford University for generously providing the ENPP1 inhibitor STF-1084.

The authors declare no competing financial interests.

Author contributions: S.SG. and K.B.E. conceived the study and wrote the manuscript. S.SG., L.T., X.S., J.T., and P.H. conducted the experiments. S.SG. analyzed the data. J.A. and M.K. contributed to the conceptualization of the study and experimental design. M.G. and R.G. performed the analysis of RNA sequencing data. V.P.W., K.B.E., and A.K. conceptualized and executed human photo testing study. All authors critically reviewed and edited the manuscript.

Figures

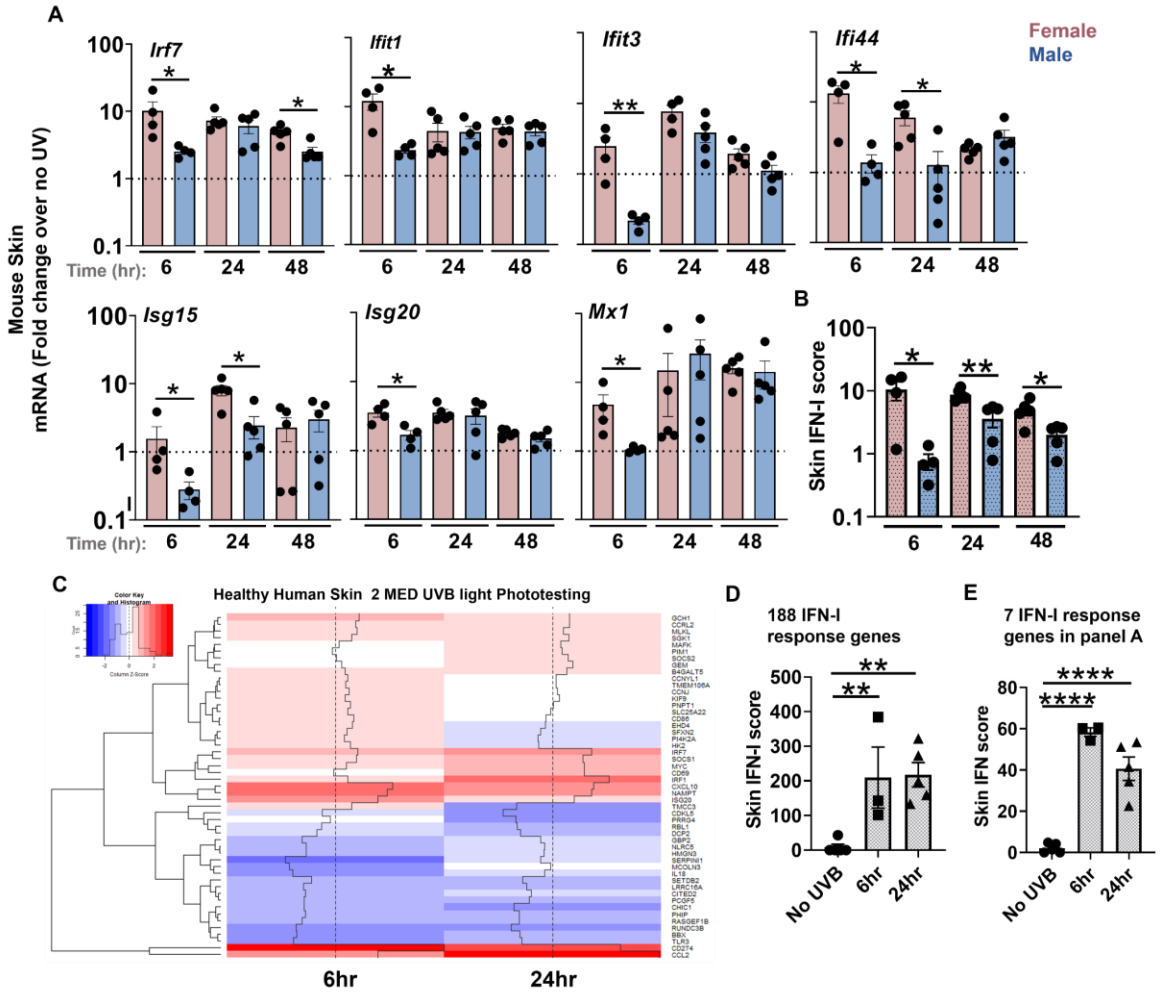

Figure 1: A single exposure of skin to UVB light triggers an early ~10-fold induction of type I IFN-stimulated genes (ISG) in female mice. Age-matched male and female B6 mice were shaved dorsally and the whole back was exposed to one dose of UVB light (500mJ/cm^2). At 6, 24, and 48 hours after UV irradiation, (**A**) fold induction in the expression of type I IFN stimulated genes (ISG) in the skin: *Irf7*, *Ifit1*, *Ifit3*, *Ifi44*, *Isg15*, *Isg20*, and *Mx1* was determined relative to baseline, i.e. non-irradiated skin. (**B**) Skin IFN scores for female and male B6 mice at 6, 24, and 48 hr after UVB light irradiation were calculated as sum of normalized expression levels of the same 7 ISG. (**C-E**) IFN-I response was evaluated in healthy human volunteers 6 and 24hr after UV exposure (2 MED UVB) and the ISG most differentially expressed shown in the heatmap (C). IFN scores were derived based on (**D**) 188 published IFN-I response genes (Der et al., 2019) or (**E**) 7 ISGs used in mouse studies (B). Statistical significance was determined by (A-B) Student's t-test (n=4-5, *p<0.05, **p<0.01) or (D-E) one-way ANOVA (n=3-5, **p<0.01, ****p<0.0001).

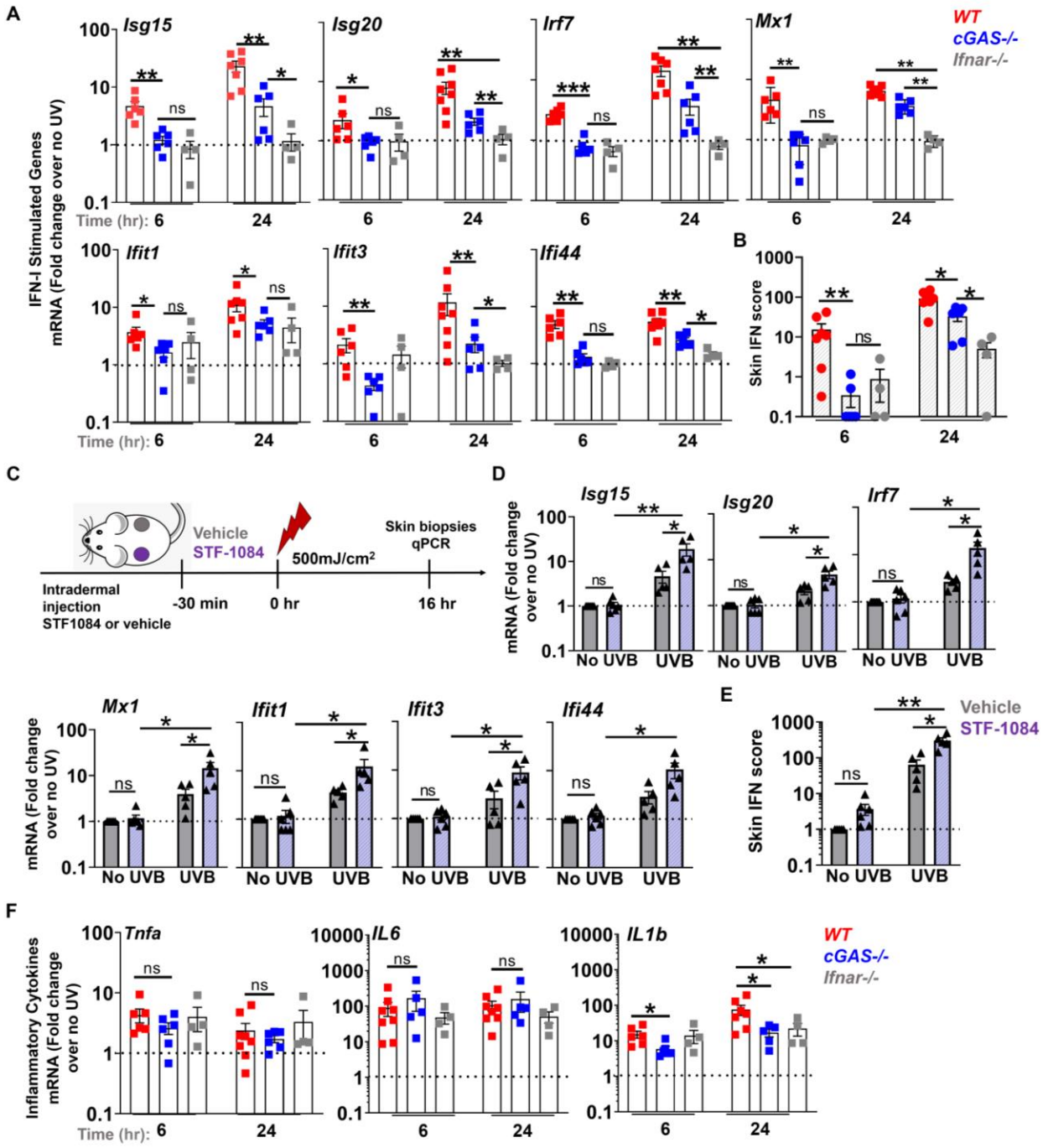

Figure 2: The early skin IFN response to UV light exposure is cGAS dependent. Age-matched female B6 (wild type, WT), *cGAS-/-*, and *Ifnar1-/-* mice were exposed to a single dose of UVB light as in Fig. 1, except that only half of the back was exposed. Skin biopsies were obtained prior to UVB light exposure and at 6 and 24hr after irradiation. (**A**) Fold change in the expression of IFN-I stimulated genes (ISG) in the skin was determined relative to baseline, i.e. non-irradiated skin. (**B**) Skin IFN scores at 6 and 24 hours after UVB were calculated as sum of normalized expression levels of the same 7 ISG. (**C**) B6 mice were shaved and treated intradermally with 100 µM ENPP1 inhibitor (STF1084) or Vehicle (PBS), 30 min prior to the

exposure to UVB light as above. Skin was biopsied 16hr after UV exposure. (**D**) Fold-change in ISG expression was determined relative to vehicle-treated non-UVB exposed skin in three treatment groups: STF1084 without UVB, vehicle with UVB, and STF-1084 with UVB (n=5, 2 independent experiments). (**F**) Fold-induction in the expression of inflammatory cytokines *Tnfa, Il-6,* and *Il1-b* were determined relative to baseline, i.e. non-irradiated skin. (A-F) Statistical significance was determined by Student's t-test (*$p<0.05$, **$p<0.01$, ***$p<0.001$, ns=not significant).

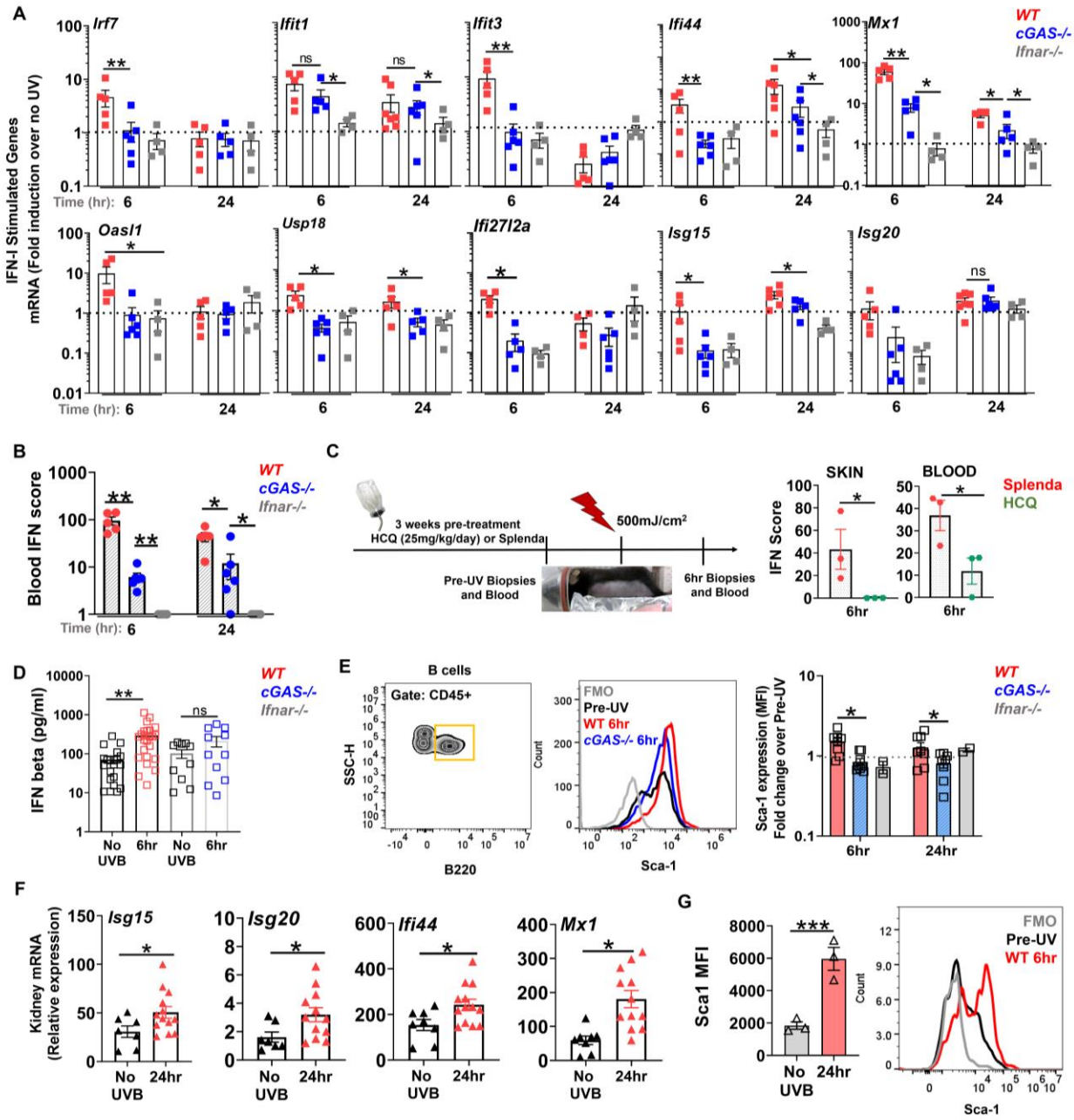

Figure 3: Acute skin exposure to UVB light triggers a systemic IFN-I response, in the presence of cGAS. Age-matched female B6 (wild type, WT), *cGAS-/-*, and *Ifnar1-/-* mice were exposed to a single dose of UVB light as in Fig. 2. (**A**) Fold induction in ISG mRNA levels in the peripheral blood cells 6 and 24hr after skin exposure to UVB light was determined relative to mRNA levels in the blood prior to UV. (**B**) Blood IFN scores for each genotype were calculated as the sum of normalized expression levels of the 7 most highly expressed ISGs after UV exposure (*Mx1, Ifit1, Ifit3, Ifi44, Usp18, Oasl1,* and *Ifi27l2a)*. (**C**) Wild type and *cGAS-/-* mice were treated with hydroxychloroquine (HCQ, 25mg/kg/day) or Splenda (controls) for 3 weeks prior to UV irradiation. Blood and skin IFN scores for both treatment groups were determined for samples prior to and 6hr after UV exposure. (**D**) IFNβ concentration in plasma prior to UV (Pre-UV) and 6hr

after UV light exposure in wild type (WT) and *cGAS-/-* mice. (**E**) Flow cytometry analysis of Sca-1 expression on B cells in the blood of wild type (WT), *cGAS-/-,* and *Ifnar-/-* mice 6 and 24hr after UVB exposure, presented as fold change relative to non-irradiated skin cells. Representative gating and histograms are shown for B cell population. (**F**) Relative expression of representative ISG transcripts in the perfused kidney tissues of wild-type mice at baseline (no UV) or 24hr after skin exposure to UVB light. (**G**) Flow cytometry analysis of Sca-1 expression on B cells in wild type (WT) perfused kidney tissue prior to and 24hr after UV exposure. Analysis of statistical significance and annotation as in Fig. 2.

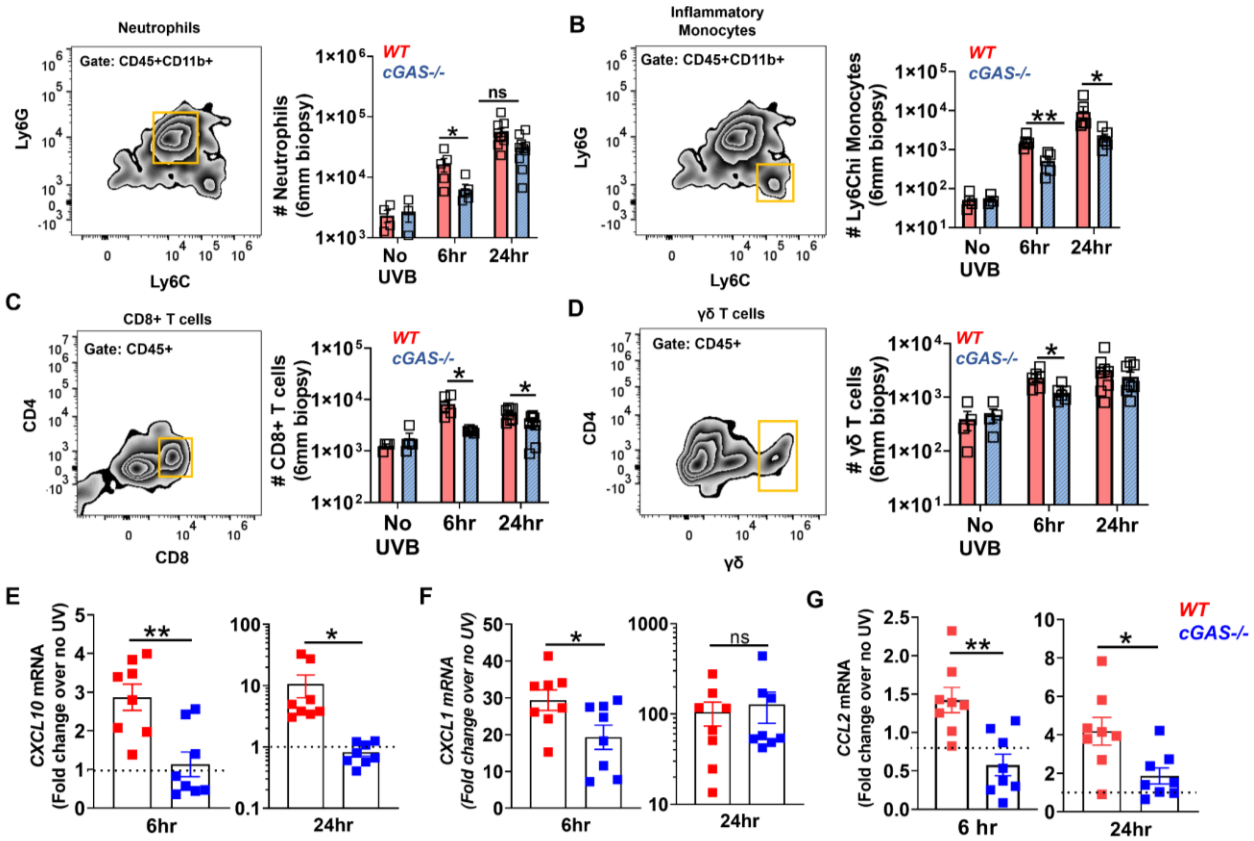

Figure 4: Skin inflammatory response to UVB light is diminished in the absence of cGAS. Age-matched female B6 (wild type, WT) and *cGAS-/-* mice were exposed to a single dose of UVB light as in Figs. 2-3. Flow cytometry analysis of skin was performed and number of (**A**) neutrophils (CD45+CD11b+Ly6C^{int}Ly6G^{hi}), (**B**) inflammatory monocytes (CD45+CD11b+Ly6C^{hi}Ly6G^{neg}), (**C**) CD8+ T cells, and (**D**) γδ+ T cells determined based on total cell number per skin biopsy (6 mm). Skin biopsies from 2-4 mice were pooled for the 6hr time point. (**E-G**) Gene expression levels of CXCL10 (E), CXCL1 (F), and CCL2 (G) in the skin were quantified by QPCR. Analysis of statistical significance and annotation as in Fig. 2.

References:

Abe, T., and G.N. Barber. 2014. Cytosolic-DNA-mediated, STING-dependent proinflammatory gene induction necessitates canonical NF-κB activation through TBK1. *J Virol* 88:5328-5341.

Ablasser, A., J.L. Schmid-Burgk, I. Hemmerling, G.L. Horvath, T. Schmidt, E. Latz, and V. Hornung. 2013. Cell intrinsic immunity spreads to bystander cells via the intercellular transfer of cGAMP. *Nature* 503:530-534.

An, J., J.J. Woodward, W. Lai, M. Minie, X. Sun, L. Tanaka, J.M. Snyder, T. Sasaki, and K.B. Elkon. 2018. Inhibition of Cyclic GMP-AMP Synthase Using a Novel Antimalarial Drug Derivative in Trex1-Deficient Mice. *Arthritis & rheumatology (Hoboken, N.J.)* 70:1807-1819.

An, J., J.J. Woodward, T. Sasaki, M. Minie, and K.B. Elkon. 2015. Cutting edge: Antimalarial drugs inhibit IFN-beta production through blockade of cyclic GMP-AMP synthase-DNA interaction. *Journal of immunology (Baltimore, Md. : 1950)* 194:4089-4093.

Ashley, C.L., A. Abendroth, B.P. McSharry, and B. Slobedman. 2019. Interferon-Independent Upregulation of Interferon-Stimulated Genes during Human Cytomegalovirus Infection is Dependent on IRF3 Expression. *Viruses* 11:246.

Baechler, E.C., F.M. Batliwalla, G. Karypis, P.M. Gaffney, W.A. Ortmann, K.J. Espe, K.B. Shark, W.J. Grande, K.M. Hughes, V. Kapur, P.K. Gregersen, and T.W. Behrens. 2003. Interferon-inducible gene expression signature in peripheral blood cells of patients with severe lupus. *Proceedings of the National Academy of Sciences of the United States of America* 100:2610-2615.

Bakhoum, S.F., B. Ngo, A.M. Laughney, J.A. Cavallo, C.J. Murphy, P. Ly, P. Shah, R.K. Sriram, T.B.K. Watkins, N.K. Taunk, M. Duran, C. Pauli, C. Shaw, K. Chadalavada, V.K. Rajasekhar, G. Genovese, S. Venkatesan, N.J. Birkbak, N. McGranahan, M. Lundquist, Q. LaPlant, J.H. Healey, O. Elemento, C.H. Chung, N.Y. Lee, M. Imielenski, G. Nanjangud, D. Pe'er, D.W. Cleveland, S.N. Powell, J. Lammerding, C. Swanton, and L.C. Cantley. 2018. Chromosomal instability drives metastasis through a cytosolic DNA response. *Nature* 553:467-472.

Barrat, F.J., T. Meeker, J. Gregorio, J.H. Chan, S. Uematsu, S. Akira, B. Chang, O. Duramad, and R.L. Coffman. 2005. Nucleic acids of mammalian origin can act as endogenous ligands for Toll-like receptors and may promote systemic lupus erythematosus. *J Exp Med* 202:1131-1139.

Bashir, M.M., M.R. Sharma, and V.P. Werth. 2009. UVB and proinflammatory cytokines synergistically activate TNF-alpha production in keratinocytes through enhanced gene transcription. *J Invest Dermatol* 129:994-1001.

Bennett, L., A.K. Palucka, E. Arce, V. Cantrell, J. Borvak, J. Banchereau, and V. Pascual. 2003. Interferon and granulopoiesis signatures in systemic lupus erythematosus blood. *J Exp Med* 197:711-723.

Bernard, J.J., C. Cowing-Zitron, T. Nakatsuji, B. Muehleisen, J. Muto, A.W. Borkowski, L. Martinez, E.L. Greidinger, B.D. Yu, and R.L. Gallo. 2012. Ultraviolet radiation damages self noncoding RNA and is detected by TLR3. *Nature medicine* 18:1286-1290.

Bethunaickan, R., and A. Davidson. 2012. Process and Analysis of Kidney Infiltrates by Flow Cytometry from Murine Lupus Nephritis. *Bio-protocol* 2:e167.

Bode, C., M. Fox, P. Tewary, A. Steinhagen, R.K. Ellerkmann, D. Klinman, G. Baumgarten, V. Hornung, and F. Steinhagen. 2016. Human plasmacytoid dentritic cells elicit a Type I Interferon response by sensing DNA via the cGAS-STING signaling pathway. *European journal of immunology* 46:1615-1621.

Bogoslowski, A., E.C. Butcher, and P. Kubes. 2018. Neutrophils recruited through high endothelial venules of the lymph nodes via PNAd intercept disseminating Staphylococcus aureus. *Proceedings of the National Academy of Sciences* 115:2449-2454.

Braunstein, I., R. Klein, J. Okawa, and V.P. Werth. 2012. The interferon-regulated gene signature is elevated in subacute cutaneous lupus erythematosus and discoid lupus erythematosus and correlates with the cutaneous lupus area and severity index score. *Br J Dermatol* 166:971-975.

Carozza, J.A., V. Boehnert, K.E. Shaw, K.C. Nguyen, G. Skariah, J.A. Brown, M. Rafat, R. von Eyben, E.E. Graves, J.S. Glenn, M. Smith, and L. Li. 2019. 2'3'-cGAMP is an immunotransmitter produced by cancer cells and regulated by ENPP1. *bioRxiv* 539312.

Catalina, M.D., P. Bachali, N.S. Geraci, A.C. Grammer, and P.E. Lipsky. 2019. Gene expression analysis delineates the potential roles of multiple interferons in systemic lupus erythematosus. *Commun Biol* 2:140-140.

Chang, A.Y., E.W. Piette, K.P. Foering, T.R. Tenhave, J. Okawa, and V.P. Werth. 2011. Response to antimalarial agents in cutaneous lupus erythematosus: a prospective analysis. *Archives of dermatology* 147:1261-1267.

Chang, J.J., M. Woods, R.J. Lindsay, E.H. Doyle, M. Griesbeck, E.S. Chan, G.K. Robbins, R.J. Bosch, and M. Altfeld. 2013. Higher expression of several interferon-stimulated genes in HIV-1-infected females after adjusting for the level of viral replication. *The Journal of infectious diseases* 208:830-838.

Chen, Q., A. Boire, X. Jin, M. Valiente, E.E. Er, A. Lopez-Soto, L. Jacob, R. Patwa, H. Shah, K. Xu, J.R. Cross, and J. Massague. 2016. Carcinoma-astrocyte gap junctions promote brain metastasis by cGAMP transfer. *Nature* 533:493-498.

Chiang, J.J., K.M.J. Sparrer, M. van Gent, C. Lassig, T. Huang, N. Osterrieder, K.P. Hopfner, and M.U. Gack. 2018. Viral unmasking of cellular 5S rRNA pseudogene transcripts induces RIG-I-mediated immunity. *Nat Immunol* 19:53-62.

Christensen, J.E., C. de Lemos, T. Moos, J.P. Christensen, and A.R. Thomsen. 2006. CXCL10 is the key ligand for CXCR3 on CD8+ effector T cells involved in immune surveillance of the lymphocytic choriomeningitis virus-infected central nervous system. *Journal of immunology (Baltimore, Md. : 1950)* 176:4235-4243.

Christou, E.A.A., A. Banos, D. Kosmara, G.K. Bertsias, and D.T. Boumpas. 2019. Sexual dimorphism in SLE: above and beyond sex hormones. *Lupus* 28:3-10.

Crow, M.K., K.A. Kirou, and J. Wohlgemuth. 2003. Microarray analysis of interferon-regulated genes in SLE. *Autoimmunity* 36:481-490.

DeLong, J.H., A.O.H. Hall, C. Konradt, G.M. Coppock, J. Park, G. Harms Pritchard, and C.A. Hunter. 2018. Cytokine- and TCR-Mediated Regulation of T Cell Expression of Ly6C and Sca-1. *The Journal of Immunology* 200:1761-1770.

Deng, L., H. Liang, M. Xu, X. Yang, B. Burnette, A. Arina, X.-D. Li, H. Mauceri, M. Beckett, T. Darga, X. Huang, T.F. Gajewski, Z.J. Chen, Y.-X. Fu, and R.R. Weichselbaum. 2014. STING-Dependent Cytosolic DNA Sensing Promotes Radiation-Induced Type I Interferon-Dependent Antitumor Immunity in Immunogenic Tumors. *Immunity* 41:843-852.

Der, E., S. Ranabothu, H. Suryawanshi, K.M. Akat, R. Clancy, P. Morozov, M. Kustagi, M. Czuppa, P. Izmirly, H.M. Belmont, T. Wang, N. Jordan, N. Bornkamp, J. Nwaukoni, J. Martinez, B. Goilav, J.P. Buyon, T. Tuschl, and C. Putterman. 2017. Single cell RNA sequencing to dissect the molecular heterogeneity in lupus nephritis. *JCI Insight* 2:e93009.

Der, E., H. Suryawanshi, P. Morozov, M. Kustagi, B. Goilav, S. Ranabathou, P. Izmirly, R. Clancy, H.M. Belmont, M. Koenigsberg, M. Mokrzycki, H. Rominieki, J.A. Graham, J.P. Rocca, N. Bornkamp, N. Jordan, E. Schulte, M. Wu, J. Pullman, K. Slowikowski, S. Raychaudhuri, J. Guthridge, J. James, J. Buyon, T. Tuschl, and C. Putterman. 2019. Tubular cell and keratinocyte single-cell transcriptomics applied to lupus nephritis reveal type I IFN and fibrosis relevant pathways. *Nat Immunol* 20:915-927.

Dunphy, G., S.M. Flannery, J.F. Almine, D.J. Connolly, C. Paulus, K.L. Jonsson, M.R. Jakobsen, M.M. Nevels, A.G. Bowie, and L. Unterholzner. 2018. Non-canonical Activation of the DNA Sensing Adaptor STING by ATM and IFI16 Mediates NF-kappaB Signaling after Nuclear DNA Damage. *Molecular cell* 71:745-760.e745.

Farkas, L., K. Beiske, F. Lund-Johansen, P. Brandtzaeg, and F.L. Jahnsen. 2001. Plasmacytoid dendritic cells (natural interferon- alpha/beta-producing cells) accumulate in cutaneous lupus erythematosus lesions. *The American journal of pathology* 159:237-243.

Feng, X., H. Wu, J.M. Grossman, P. Hanvivadhanakul, J.D. FitzGerald, G.S. Park, X. Dong, W. Chen, M.H. Kim, H.H. Weng, D.E. Furst, A. Gorn, M. McMahon, M. Taylor, E. Brahn, B.H. Hahn, and B.P. Tsao. 2006. Association of increased interferon-inducible gene expression with disease activity and lupus nephritis in patients with systemic lupus erythematosus. *Arthritis and rheumatism* 54:2951-2962.

Foering, K., R. Goreshi, R. Klein, J. Okawa, M. Rose, A. Cucchiara, and V.P. Werth. 2012. Prevalence of self-report photosensitivity in cutaneous lupus erythematosus. *J Am Acad Dermatol* 66:220-228.

Gaidt, M.M., T.S. Ebert, D. Chauhan, K. Ramshorn, F. Pinci, S. Zuber, F. O'Duill, J.L. Schmid-Burgk, F. Hoss, R. Buhmann, G. Wittmann, E. Latz, M. Subklewe, and V. Hornung. 2017. The DNA Inflammasome in Human Myeloid Cells Is Initiated by a STING-Cell Death Program Upstream of NLRP3. *Cell* 171:1110-1124.e1118.

Gehrke, N., C. Mertens, T. Zillinger, J. Wenzel, T. Bald, S. Zahn, T. Tuting, G. Hartmann, and W. Barchet. 2013. Oxidative damage of DNA confers resistance to cytosolic nuclease TREX1 degradation and potentiates STING-dependent immune sensing. *Immunity* 39:482-495.

Gentleman, R.C., V.J. Carey, D.M. Bates, B. Bolstad, M. Dettling, S. Dudoit, B. Ellis, L. Gautier, Y. Ge, J. Gentry, K. Hornik, T. Hothorn, W. Huber, S. Iacus, R. Irizarry, F. Leisch, C. Li, M. Maechler, A.J. Rossini, G. Sawitzki, C. Smith, G. Smyth, L. Tierney, J.Y. Yang, and J. Zhang. 2004. Bioconductor: open software development for computational biology and bioinformatics. *Genome biology* 5:R80.

Green, R., R.C. Ireton, and M. Gale, Jr. 2018. Interferon-stimulated genes: new platforms and computational approaches. *Mammalian genome : official journal of the International Mammalian Genome Society* 29:593-602.

Hamilton, J.A., Q. Wu, P. Yang, B. Luo, S. Liu, H. Hong, J. Li, M.R. Walter, E.N. Fish, H.C. Hsu, and J.D. Mountz. 2017. Cutting Edge: Endogenous IFN-beta Regulates Survival and Development of Transitional B Cells. *Journal of immunology (Baltimore, Md. : 1950)* 199:2618-2623.

Hamilton, J.A., Q. Wu, P. Yang, B. Luo, S. Liu, J. Li, L.M. A, I. Sanz, W.W. Chatham, H.C. Hsu, and J.D. Mountz. 2018. Cutting Edge: Intracellular IFN-beta and Distinct Type I IFN Expression Patterns in Circulating Systemic Lupus Erythematosus B Cells. *Journal of immunology (Baltimore, Md. : 1950)* 201:2203-2208.

Harding, S.M., J.L. Benci, J. Irianto, D.E. Discher, A.J. Minn, and R.A. Greenberg. 2017. Mitotic progression following DNA damage enables pattern recognition within micronuclei. *Nature* 548:466-470.

Kemp, M.G., L.A. Lindsey-Boltz, and A. Sancar. 2015. UV Light Potentiates STING (Stimulator of Interferon Genes)-dependent Innate Immune Signaling through Deregulation of ULK1 (Unc51-like Kinase 1). *The Journal of biological chemistry* 290:12184-12194.

Li, A., M. Yi, S. Qin, Y. Song, Q. Chu, and K. Wu. 2019. Activating cGAS-STING pathway for the optimal effect of cancer immunotherapy. *Journal of Hematology & Oncology* 12:35.

Li, L., Q. Yin, P. Kuss, Z. Maliga, J.L. Millan, H. Wu, and T.J. Mitchison. 2014. Hydrolysis of 2'3'-cGAMP by ENPP1 and design of nonhydrolyzable analogs. *Nature chemical biology* 10:1043-1048.

Li, T., and Z.J. Chen. 2018. The cGAS–cGAMP–STING pathway connects DNA damage to inflammation, senescence, and cancer. *The Journal of Experimental Medicine* 215:1287-1299.

Liang, Y., L.C. Tsoi, X. Xing, M.A. Beamer, W.R. Swindell, M.K. Sarkar, C.C. Berthier, P.E. Stuart, P.W. Harms, R.P. Nair, J.T. Elder, J.J. Voorhees, J.M. Kahlenberg, and J.E. Gudjonsson. 2017. A gene network regulated by the transcription factor VGLL3 as a promoter of sex-biased autoimmune diseases. *Nat Immunol* 18:152-160.

Liu, J., F. Li, Y. Ping, L. Wang, X. Chen, D. Wang, L. Cao, S. Zhao, B. Li, P. Kalinski, S.H. Thorne, B. Zhang, and Y. Zhang. 2015. Local production of the chemokines CCL5 and CXCL10 attracts CD8+ T lymphocytes into esophageal squamous cell carcinoma. *Oncotarget* 6:24978-24989.

Lood, C., L.P. Blanco, M.M. Purmalek, C. Carmona-Rivera, S.S. De Ravin, C.K. Smith, H.L. Malech, J.A. Ledbetter, K.B. Elkon, and M.J. Kaplan. 2016. Neutrophil extracellular traps enriched in oxidized mitochondrial DNA are interferogenic and contribute to lupus-like disease. *Nature medicine* 22:146-153.

Ng, C.T., J.L. Mendoza, K.C. Garcia, and M.B.A. Oldstone. 2016. Alpha and Beta Type 1 Interferon Signaling: Passage for Diverse Biologic Outcomes. *Cell* 164:349-352.

Ohkuri, T., A. Ghosh, A. Kosaka, J. Zhu, M. Ikeura, M. David, S.C. Watkins, S.N. Sarkar, and H. Okada. 2014. STING contributes to antiglioma immunity via triggering type I IFN signals in the tumor microenvironment. *Cancer Immunol Res* 2:1199-1208.

Patra, V., K. Wagner, V. Arulampalam, and P. Wolf. 2019. Skin Microbiome Modulates the Effect of Ultraviolet Radiation on Cellular Response and Immune Function. *iScience* 15:211-222.

Pogue, S.L., B.T. Preston, J. Stalder, C.R. Bebbington, and P.M. Cardarelli. 2004. The receptor for type I IFNs is highly expressed on peripheral blood B cells and monocytes and mediates

a distinct profile of differentiation and activation of these cells. *Journal of interferon & cytokine research : the official journal of the International Society for Interferon and Cytokine Research* 24:131-139.

Psarras, A., A. Alase, A. Antanaviciute, I.M. Carr, M.Y. Md Yusof, M. Wittmann, P. Emery, G.C. Tsokos, and E.M. Vital. 2018. Plasmacytoid dendritic cells are functionally exhausted while non-haematopoietic sources of type I interferon dominate human autoimmunity. *bioRxiv* 502047.

Sarkar, M.K., G.A. Hile, L.C. Tsoi, X. Xing, J. Liu, Y. Liang, C.C. Berthier, W.R. Swindell, M.T. Patrick, S. Shao, P.S. Tsou, R. Uppala, M.A. Beamer, A. Srivastava, S.L. Bielas, P.W. Harms, S. Getsios, J.T. Elder, J.J. Voorhees, J.E. Gudjonsson, and J.M. Kahlenberg. 2018. Photosensitivity and type I IFN responses in cutaneous lupus are driven by epidermal-derived interferon kappa. *Annals of the rheumatic diseases* 77:1653-1664.

Schuch, A.P., N.C. Moreno, N.J. Schuch, C.F.M. Menck, and C.C.M. Garcia. 2017. Sunlight damage to cellular DNA: Focus on oxidatively generated lesions. *Free Radical Biology and Medicine* 107:110-124.

Sharma, M.R., B. Werth, and V.P. Werth. 2011. Animal models of acute photodamage: comparisons of anatomic, cellular and molecular responses in C57BL/6J, SKH1 and Balb/c mice. *Photochemistry and photobiology* 87:690-698.

Shipman, W.D., S. Chyou, A. Ramanathan, P.M. Izmirly, S. Sharma, T. Pannellini, D.C. Dasoveanu, X. Qing, C.M. Magro, R.D. Granstein, M.A. Lowes, E.G. Pamer, D.H. Kaplan, J.E. Salmon, B.J. Mehrara, J.W. Young, R.M. Clancy, C.P. Blobel, and T.T. Lu. 2018. A protective Langerhans cell-keratinocyte axis that is dysfunctional in photosensitivity. *Science translational medicine* 10:

Smyth, G.K. 2004. Linear models and empirical bayes methods for assessing differential expression in microarray experiments. *Statistical applications in genetics and molecular biology* 3:Article3.

Sontheimer, C., D. Liggitt, and K.B. Elkon. 2017. Ultraviolet B Irradiation Causes Stimulator of Interferon Genes-Dependent Production of Protective Type I Interferon in Mouse Skin by Recruited Inflammatory Monocytes. *Arthritis & rheumatology (Hoboken, N.J.)* 69:826-836.

Swanson, K.V., R.D. Junkins, C.J. Kurkjian, E. Holley-Guthrie, A.A. Pendse, R. El Morabiti, A. Petrucelli, G.N. Barber, C.A. Benedict, and J.P.-Y. Ting. 2017. A noncanonical function of cGAMP in inflammasome priming and activation. *The Journal of Experimental Medicine* 214:3611-3626.

Vanpouille-Box, C., A. Alard, M.J. Aryankalayil, Y. Sarfraz, J.M. Diamond, R.J. Schneider, G. Inghirami, C.N. Coleman, S.C. Formenti, and S. Demaria. 2017. DNA exonuclease Trex1 regulates radiotherapy-induced tumour immunogenicity. *Nature communications* 8:15618-15618.

Vatner, R.E., and E.M. Janssen. 2019. STING, DCs and the link between innate and adaptive tumor immunity. *Molecular Immunology* 110:13-23.

Wang, H., S. Hu, X. Chen, H. Shi, C. Chen, L. Sun, and Z.J. Chen. 2017. cGAS is essential for the antitumor effect of immune checkpoint blockade. *Proceedings of the National Academy of Sciences* 201621363.

Wolf, S.J., S.N. Estadt, J. Theros, T. Moore, J. Ellis, J. Liu, T.J. Reed, C.O. Jacob, J.E. Gudjonsson, and J.M. Kahlenberg. 2019. Ultraviolet light induces increased T cell activation in lupus-

prone mice via type I IFN-dependent inhibition of T regulatory cells. *Journal of autoimmunity* 103:102291.

Wu, J., L. Sun, X. Chen, F. Du, H. Shi, C. Chen, and Z.J. Chen. 2013. Cyclic GMP-AMP is an endogenous second messenger in innate immune signaling by cytosolic DNA. *Science* 339:826-830.

Yamazaki, S., M. Odanaka, A. Nishioka, S. Kasuya, H. Shime, H. Hemmi, M. Imai, D. Riethmacher, T. Kaisho, N. Ohkura, S. Sakaguchi, and A. Morita. 2018. Ultraviolet B-Induced Maturation of CD11b-Type Langerin(-) Dendritic Cells Controls the Expansion of Foxp3(+) Regulatory T Cells in the Skin. *Journal of immunology (Baltimore, Md. : 1950)* 200:119-129.

Zeidi, M., H.J. Kim, and V.P. Werth. 2019. Increased Myeloid Dendritic Cells and TNF-alpha Expression Predicts Poor Response to Hydroxychloroquine in Cutaneous Lupus Erythematosus. *J Invest Dermatol* 139:324-332.

Zevini, A., D. Olagnier, and J. Hiscott. 2017. Crosstalk between Cytoplasmic RIG-I and STING Sensing Pathways. *Trends in immunology* 38:194-205.